Hydrolysis optimization of mannan, curdlan and cell walls from *Endomyces fibuliger* grown in mussel processing wastewaters

Miguel Angel Prieto*, José Antonio Vázquez & Miguel Anxo Murado

Grupo de Reciclado y Valorización de Materiales Residuales (REVAL)
Instituto de Investigacións Mariñas (CSIC)
r/Eduardo Cabello, 6. Vigo-36208, Galicia, Spain
*Author to whom correspondence should be addressed
E-Mail: michaelumangelum@iim.csic.es
Tel.: +34986214469; +34986231930
Fax: +34986292762

ABSTRACT

The aim of this report was to optimize the hydrolysis of the cell walls (CWs) from the yeast *Endomyces fibuliger* grown in mussel processing wastewaters (MPW) to establish a more accurate protocol for analyzing the composition of the monosaccharides in these CWs. Therefore, a kinetic study of CW hydrolysis and polysaccharide standards (mannan and curdlan) was performed to determine the effect of different temperatures and trifluoroacetic acid (TFA) concentrations on this process. In all cases, the experimental data were fit satisfactorily to Saeman's equation with an Arrhenius relation between rate constants and the temperature effect. Optimal conditions for curdlan and mannan hydrolysis were achieved with 70% TFA at 100ºC for 2.3 h and 50% TFA at 100ºC for 2.6 h, respectively. The best operating options for CW hydrolysis were 100ºC/70% TFA for 4.58 h, 100ºC/50% TFA for 4.08 h and 100ºC/70% TFA for 3.27 h for the maximum production of glucose, mannose and reducing sugars, respectively.

Keywords: yeast cell walls; mussel processing wastes; *Endomyces fibuliger*; trifluoroacetic acid hydrolysis; mathematical modeling; curdlan and mannan

1. Introduction

Cell walls (CWs) in yeast and fungi are dynamic, stratified structures that are in a constant state of hydrolysis, and its biosynthesis is controlled by strict regulation. Changes in culture conditions, different cellular stages and dimorphic transitions can influence the CW composition [1]. The main components of CWs are 1) structural elements such as β-1,3 and β-1,6 glucans (a polymer of D-glucose) and chitin (a polymer of N-acetylglucosamine), 2) matrix components, such as α-glucans and glyco- or mannoproteins (polymers of mannose linked to proteins), and 3) lipids and proteins [2-4].

55 The study of active oligosaccharides and β-glucans has generated much interest over the last
56 two decades because of the substantial empirical evidence that they have healthy effects,
57 mainly as antitumor and immunomodulation agents, on different biological entities that range
58 from invertebrates to mammals [5-7]. Although the mechanisms that underlie these properties
59 are still not completely understood, it seems clear that β-glucans activate the leukocyte
60 mediators of the immune response [8], acting as an antigenic stimulus of dendrite cells and/or
61 developing the phagocytic activity of the leukocytes [9]. Their effects mainly depend on the
62 molecular weight, degree of polymerization, proportion of 1-3, 1-4 and 1-6 bonds, presence of
63 mannose and the formation of chitin or protein complexes [10]. For the latter case, there is
64 still no clear consensus, but it is generally agreed that chitin and mannoprotein complexes
65 develop the appropriate properties and also that a high molecular weight (low solubility)
66 produces adverse effects, at least when intraperitoneal administration is used. Additionally,
67 these factors are modified by the type of producer microorganism, the taxonomic group, the
68 life-cycle phase and the medium growth conditions [1]. Therefore, it is important to have
69 tools to identify and quantify the carbohydrates (i.e., polysaccharides of mannose, glucose and
70 N-acetyl-D-glucosamine) in microbial CW.
71
72 The most common methods for studying the composition of these carbohydrates are based on
73 chromatography techniques (e.g., gas chromatography (GC) or high-performance liquid
74 chromatography (HPLC)), which allow the CW monosaccharides to be distinguished. In these
75 techniques an initial hydrolysis step, based on a chemical reaction in acid media at high
76 temperatures, is necessary [11,12]. This step is a destructive process and its effects depend on
77 the structure, the CW composition and the conditions and type of chemical used [13,14].
78 Optimum hydrolysis conditions should maximize polysaccharide breakdown and minimize
79 the destruction of the corresponding released monosaccharides. Therefore, we need to
80 consider that monosaccharide stability with strong acids employed for hydrolysis varies
81 depending on their chemical composition and the presence and proportion of amino groups.

Nevertheless, in the literature, there is a tendency to accept the optimal hydrolysis conditions used in one system for another. For example, using the conditions found in potato peel for the structural analysis of yeast CW carbohydrates in [13]. Using non-optimal procedures for these substrates leads to the partial destruction of some monosaccharides or the incomplete hydrolysis of the polysaccharides, which alters the final compositional results. It is therefore essential to optimize the hydrolysis conditions and study the joint effects of variables such as temperature and the oxidant compound for each substrate used to study its carbohydrate composition. To our knowledge, the optimal conditions for breaking down curdlan, mannan and yeast CW have not yet been reported.

The CWs of different yeasts have been used as substrates for β-glucans production [2,6]. The most common is *Saccharomyces cereviseae*; however, amylolytic yeasts, which are able to grow in amylaceous and residual effluents, have not yet been studied as polysaccharides and β-glucans producers. The benefit of this proposal is especially interesting in our region because more than 25% of the world mussel production occurs on the Galician coast (NW, Spain). In the thermal process for canning mussels, approximately 1.6 million m^3 of mussel processing wastewaters (MPW) are generated per year and dumped in the sea without previous depuration [16]. This residual effluent has been successfully used as a carbon substrate for several bioproductions including gibberellins [17], amylases [18], glucose oxidase [19], citric acid [20], pediocin [21], hyaluronic acid [22] and single cell proteins from *Endomyces fibuliger* [23]. This last amylolytic yeast is an excellent candidate for glucans production because its CW composition (i.e., 56% CW per biomass unit with 64% of total sugars per CW unit) obtained in our study is higher than that of other yeasts (i.e., 35% per biomass unit with 85% total sugars per CW unit) commonly used for this purpose and as reported in [24]. To our knowledge, *E. fibuliger* has not been previously studied for this purpose.

The main objective of this study was to investigate the effect of temperature and trifluoroacetic acid (TFA) concentration on the hydrolysis kinetics of commercial curdlan and mannan and CWs obtained from *Endomyces fibuliger* that was previously grown in MPW. These findings are essential for accurately quantifying CW monosaccharides. The experimental profiles were fit satisfactorily to the Saeman and Arrhenius equations for describing and defining the optimal conditions for the maximal breakdown of polysaccharides to monosaccharides and minimizing the destruction of these monosaccharides due to the thermal and chemical reactions.

2. Materials and Methods

2.1. Microbiological methods, media preparation and culture conditions

Endomyces fibuliger (CBS 2521) was used as the CW source in this study. MPW were kindly supplied by Marcelino S.A. (Galicia, Spain), and their chemical composition was as follows: 7 g/L glycogen, 0.10 g/L reducing sugars, 3.5 g/L proteins and 1.6 g/L total nitrogen. Sediments were not observed in these effluents, and the initial pH was 7.2.

To precipitate the proteins, the MPW was first treated with HCl (50% v/v) until a pH of 4.5 was reached, and the supernatant was subsequently concentrated with an ultrafiltration membrane [25,26]. Ultrafiltration was performed using 0.56 m^2 spiral polyethersulfone membranes (*Millipore Prepscale*) with a 100 kDa cutoff using an assembly with total recirculation at 30ºC.

This concentrate, which contained 25 g/L of glycogen and 2 g/L of protein-Lowry, was supplemented with 400 mg/L of phosphorus (KH_2PO_4) and 1200 mg/L of nitrogen ($NaNO_3$:NH_4Cl in a 0.8:0.2 (w/w) ratio) to formulate the MPW based medium for yeast fermentation [23,27]. The kinetic analysis cultures were performed in triplicate in 300 mL Erlenmeyer flasks with 50 mL of medium at 30ºC, 200 rpm and an initial pH of 5.0. For the

biomass and CW studies, 3 L flasks with 500 mL of culture medium were collected at the end of the growth phase (55 h). Inocula (2%, v/v), a cellular suspension of 48 h-old *E. fibuliger* fermentations in MPW based medium, were prepared to a final concentration of 2.5×10^6 cells/mL in the experimental units.

2.2. Fermentation sampling and analytical determinations

At pre-established times, each Erlenmeyer flask was removed from the shaker incubator and the post-incubation medium was centrifuged at 4500 g for 20 min. The sediment was washed using distilled water and centrifuged again to eliminate all medium components. The washed precipitate was used to determine the dry weight after it had been dried in an oven at 107ºC. The following compounds were analyzed in the supernatant: total amylolytic activity [18], total sugars [28,29], proteins [30], total nitrogen [31] and reducing sugars [32].

The 3 L flasks were collected at 55 h and the fermented media were centrifuged at 10,000 g for 20 min. The sediment was separated by filtration using 0.45 μm glass microfiber filters (Whatman), washed with abundant distilled water, lyophilized and crushed with a pestle to determine its chemical composition. The obtained material was stored at -20ºC after desiccation with KOH for CW treatment. The total sugars, reducing sugars, total nitrogen, ash (by calcination at 550ºC until constant weight) and total lipids using Soxhlet extraction were determined in triplicate [33]. The CWs were obtained according to the methodology proposed by Kasahara [34]. However, the polysaccharides standards used as controls for the hydrolysis process, curdlan and mannan, were purchased from Sigma Aldrich (St. Louis, MO, USA).

2.3. Hydrolysis conditions and hydrolysates analysis

The substrates, CWs and polysaccharide standards were placed in 30 mL tubes with sealed Teflon caps and mixed with several diluted TFA concentrations that ranged from 10% to 70% (v/v) at different temperatures between 35 and 120ºC with an initial solid/liquid ratio of 0.5

mg/mL. Samples were removed from the reaction media at the pre-established times. After hydrolysis and before the chemical analysis, the TFA was completely evaporated, and the hydrolysates were completely dried in a heating oven with a gas extractor for between 30 and 50 h at 30ºC.

The amount of monosaccharides released by hydrolysis was determined using the following:

1) The 3,5-dinitrosalicylic reaction method, with spectrophotometric measurements taken at 540 nm for the hydrolysis of the standards and the CWs [32]
2) Gas chromatography-mass spectrometry (GC-MS) measuring alditol derivatives (only in the case of CW) to differentiate between the release of mannose and glucose [35].

This second method is based on forming alditol acetate compounds from monosaccharides present in the CWs and then quantifying GC with a flame ionization detector. Thus, 3 mL of pyridine anhydride (C_6H_5N) and 1 mL of acetic anhydride ($CH_3CO_2CH_3$) were added to 1 mg of the sample in solution (generating a reductive ambient), and the oxygen was removed by nitrogen flow. The reaction medium was agitated for 24 h at room temperature. Next, 3 mL of concentrated HCl was added drop by drop in an ice bath. The resulting phase was extracted with ethyl acetate three times until a volume of 5 mL was reached. The calibration curves of the monosaccharides (i.e., glucose and mannose) were prepared as pentacetates [36] using ribose obtained by the same procedure as the internal standard.

We used an HP 5850 GC with a selective mass detector HP 5971 (series J) in scan mode in the range 50-400 m/z, and a Supelco SP-2330 column (30 m × 0.25 mm). The temperatures were 200ºC (injector), 280ºC (detector), and a column programming range from 150ºC to 250ºC, which was maintained for 10 min, with a gradient of 7ºC/min. Helium was used as the carrier gas and its flow was kept constant at 8 psi.

190

191 *2.4. Mathematical models*

192 The mathematical equation used to describe the experimental hydrolysis profiles was based
193 on a pseudohomogeneous kinetic model in liquid phase with a first order reaction [37,38],
194 according to the modifications reported in [39] and the variables studied in our report:

195

196 $$Polysaccharide \xrightarrow{k_h} Monosaccharide \xrightarrow{k_d} Decomposition\ products$$

197

198 where k_h is the specific rate of monosaccharide production (h^{-1}) and k_d is the specific
199 decomposition rate (h^{-1}). Integrating the corresponding differential equations led to the
200 following explicit equation:

201

202 $$M = M_0 e^{-k_d t} + P_0 \frac{k_h}{k_d - k_h}(e^{-k_h t} - e^{-k_d t}) \quad (1)$$

203

204 where t is the time course of the reaction (min), M is the relative concentration of
205 monosaccharide, glucose or mannose (%), M_0 is the initial concentration of the
206 monosaccharide (%) and P_0 is the initial concentration of the polysaccharide (%). This
207 equation was used to model the hydrolysis of the polysaccharide standards and the CWs from
208 *E. fibuliger* in all the experimental conditions tested. The sugar values from the
209 polysaccharide standards were calculated in relation to the maximum sugar concentration
210 measured (in %). For *E. fibuliger* bioproduction, the sugar values were calculated in terms of
211 the CW dry weight for each instance.

212

213 In all cases, M_0 was zero, and thus equation (1) is simplified to:

214

$$M = P_0 \frac{k_h}{k_d - k_h}(e^{-k_h t} - e^{-k_d t}) \quad (2)$$

The time necessary to obtain maximal monosaccharide production (t_m, in hours) was calculated by deriving equation (2) with respect to time and equaling to zero:

$$\left.\frac{dM}{dt}\right|_{t=t_m} = P_0 \frac{k_h}{k_d - k_h}(-k_h e^{-k_h t} + k_d e^{-k_d t}) = 0 \Rightarrow t_m = \frac{\ln\left(k_d / k_h\right)}{k_d - k_h} \quad (3)$$

If t_m is substituted in equation (2), we can obtain the maximum monosaccharide production (M_m, in %):

$$M_m = P_0 \frac{k_h}{k_d - k_h}(e^{-k_h t_m} - e^{-k_d t_m}) \quad (4)$$

The temperature dependence of the kinetic parameters from equation (1) is described by the Arrhenius equation:

$$k_i = k_{i0} \exp\left(-\frac{Ea_i}{RT}\right) \quad (5)$$

where k_i is the kinetic parameter (for $i = h$ or d), k_{i0} is the pre-exponential factor (h^{-1}), Ea_i is the activation energy (kJ/mol), R is the universal gas constant (8.314×10^{-3} kJ mol^{-1} K^{-1}) and T is the absolute temperature (K).

By inserting equation (5) into equation (2), a bivariate model is used to calculate the activation energies, the pre-exponential factors and the relative concentration of monosaccharide (M) at any given time and temperature:

239 $$M = P_0 \frac{k_{h0}\exp\left(-\frac{Ea_h}{RT}\right)}{k_{d0}\exp\left(-\frac{Ea_d}{RT}\right) - k_{h0}\exp\left(-\frac{Ea_h}{RT}\right)}\left[\exp\left(-k_{h0}\exp\left(-\frac{Ea_h}{RT}\right)t\right) - \exp\left(-k_{d0}\exp\left(-\frac{Ea_d}{RT}\right)t\right)\right] \quad (6)$$

240

241 *2.5. Numerical and statistical methods*

242 The strategy for modeling the experimental data is summarized in the following steps:

243

244 1) Experimental data from each individual set of TFA and temperature were fit to equation
245 (2). Because P_0 has to be equal for each substrate independently of the TFA and temperature
246 conditions, a numerical estimate of this parameter was made only and jointly for all
247 experimental series. The individual set of parameters (k_h and k_d) obtained for each TFA and
248 temperature condition was used to calculate the monosaccharide production maximum and the
249 time it occurs (equations 4 and 3, respectively).

250

251 2) The experimental data from each TFA concentration set at all tested temperatures were fit
252 jointly to equation (6) to obtain the numerical values of Ea_h, k_{h0}, Ea_d and k_{d0}. The used P_0
253 value was that obtained in previous adjustments.

254

255 The fitting procedures and parametric estimates from the experimental results were performed
256 by minimizing the sum of quadratic differences between the observed and model-predicted
257 values using the nonlinear least-squares (quasi-Newton) method provided by the 'Solver'
258 macro from Microsoft Excel spreadsheet. The confidence intervals of the best-fit values for
259 the parametric estimates (α=0.05), consistency of the mathematical models (Fisher's F test;
260 p<0.05) and covariance and correlation matrices were calculated using the 'SolverAid' macro,
261 which is freely available from de Levie's Excellaneous website:
262 http://www.bowdoin.edu/~rdelevie/excellaneous/.

263

3. Results and Discussion

3.1. E. fibuliger culture and biomass composition

Figure 1 shows the experimental results of *E. fibuliger* fermentation in the MPW-based medium. Maximum growth was obtained at 55 h with 12 g/L of biomass (as dry weight). At that time, the glycogen from in residual culture media was completely consumed, and the pH increased from 5.3 to 6.8. At 30 h, the yeast amylases were deactivated due to a drop in the reducing sugar concentration. In addition, the yeast consumed 1.3 g/L of protein-Lowry. Therefore, 55 h of culture was selected to obtain the maximum biomass. This biomass was then used for compositional analyses and CW hydrolysis.

The chemical composition of the biomass after 55 h of cultivation was as follows (in %, dry basis (db)): 59.2 ± 2.5 total sugars, 7.63 ± 0.77 reducing sugars, 14.9 ± 0.7 total lipids, 1.6 ± 0.2 ash and 6.4 ± 0.4 proteins (as N × 6.25). The values for the CW analysis were the following (in %, db): 69.3 ± 1.2 total sugars, 25.9 ± 1.4 proteins, 0.7 ± 0.1 total lipids and 3.3 ± 0.2 ash. Reducing sugars were undetected in the CWs. A 54.7% CW yield was obtained from the *E. fibuliger* biomass. This value was higher than that reported in [24]. In this article, the yeasts *Kluyveromyces marxianus* and *Debaryomyces hansenii* had the highest proportion of CW in their biomass (32.5% and 32%, respectively). However, in all the microorganisms studied by these authors, the total sugars percentage was superiors to the *E. fibuliger* results (more than 84% compared with 65% for *E. fibuliger*). These differences could be due to the different methods for obtaining CWs. Using autoclaving, a French pressure cell press, cell lysis by glass beads or a homogenizer led to different efficiency results and yields in the biomass breakdown of microorganisms [24].

3.2. Hydrolysis kinetics of curdlan and mannan

The hydrolysis results at different temperatures and several TFA concentrations using curdlan and mannan as substrates are shown in Figure 2. The profiles adjusted to the experimental

291 data according to model (2) are also shown. Table 1 lists the values of the kinetic parameters
292 and the statistical analyses of the numerical fittings. In general, the proposed models were
293 statistically robust (Fisher's F-test *p*-values < 0.05), the parametric estimations were
294 significant (Student's t-test α = 0.05), the residuals were randomly distributed and
295 autocorrelations were not observed by the Durbin-Watson test (data not shown). The linear
296 determination coefficients (R^2) between the predicted and observed values were always
297 greater than 0.95.
298
299 Table 2 summarizes the parameters defined by equations (3) and (4), which are important for
300 determining the optimal conditions for maximal sugar release from commercial
301 polysaccharides or monosaccharide extraction from CW for chemical composition analysis.
302 Using curdlan as the hydrolysis substrate, four different experimental conditions, 80ºC/70%
303 TFA, 80ºC/50% TFA, 100ºC/70% TFA and 100ºC/50% TFA, were used to obtain the
304 maximum concentrations of released glucose (98.42%, 94.76%, 94.10% and 94.23%,
305 respectively), though with markedly different maximum hydrolysis times (10.7 h, 14.2 h, 2.3
306 h and 3.4 h, respectively). To shorten the processing time, we performed the hydrolysis at
307 100ºC and 70% TFA, although almost 4% less glucose is produced under these conditions.
308 Mannan hydrolysis demonstrated two optimal maxima in the 100ºC/50% TFA and 80ºC/50%
309 TFA pairs with processing times of 2.6 h and 13.1 h, respectively, and the former option is the
310 most useful. The decreased t_m was correlated by increasing the TFA concentration but without
311 a clear tendency for significant modeling.
312
313 These results are in agreement with those previously reported by Freimund et al. [14]. These
314 authors obtained the best conditions for glucan hydrolysis in the range of 92.5 to 100ºC for
315 1.5 to 3 h and 72.5% TFA. For breaking down mannan, these intervals were 90 to 100ºC for
316 1.75 to 4 h and with a higher TFA concentration (60%) than we propose. Although [14]
317 presents a similar study of the combined effect of the dependent variables (i.e., temperature,

time and acid concentration), these data were obtained by individual observation and by combining the variables at their apparent maximum point without optimizing by mathematical modeling. This type of procedure is common in the literature, but it leads to a faulty understanding of the combined variable effect in terms of the response to maximization [40,41].

The numerical parameters for the bivariate equation (6) are shown in Table 3. In both hydrolysis and decomposition, the activation energies for curdlan were higher than that for mannan, which is in agreement with the shorter t_m obtained for this polysaccharide (Table 2). In addition, the increase in the TFA concentration led to a slight decrease in Ea_h and Ea_d. Indeed, with higher acidity in the reaction medium, less energy is needed to break the glycosidic bonds that link the monosaccharides in the polysaccharide skeleton.

3.3. E. fibuliger CW hydrolysis kinetics

Figure 3 shows the experimental data and modeling trends of the hydrolysis kinetics of the CWs produced by *E. fibuliger*. The statistical analyses of the relevant kinetic parameters are summarized in Table 4. The P_0 values were 59.4%, 41% and 24.5% for the ratios of RS, glucose and mannose per CW db, respectively. These percentages were similar to those reported earlier in section 3.1 (i.e., 69.3% total sugars). All of the parameters were again statistically significant (Student's t-test, α=0.05), and equation (2) was consistent (Fisher's F-test, α=0.05 and R^2).

Equations (3) and (4) permitted us to predict the hydrolysis time (t_m) necessary for obtaining the maximum percentages of glucose, mannose and reducing sugars released from the studied yeast CWs (Table 5). There were two options for recovering the maximum glucose: 100ºC/70% TFA and 120ºC/70% TFA, with reaction times of 4.58 h and 0.88 h, respectively. These conditions were different for mannose: 100ºC/50% TFA for 4.08 h, 120ºC/35% TFA

345 for 1 h and 120ºC/50% TFA for 0.83 h. Therefore, the suggestion by Freimund et al. (2005)
346 that for determining the monosaccharides present in the CWs, different treatment conditions
347 should be applied seems reasonable. For compositional analyses of glucose and mannose in *E.*
348 *fibuliger* CWs, we suggest the following operating conditions: 100ºC/70% TFA for 4.58 h and
349 100ºC/50% TFA for 4.08 h, respectively. The reducing sugars results show that maximum RS
350 production is obtained at 100ºC with 70% TFA for 3.27 h. However, if shorter processing
351 times are necessary, the hydrolysis reaction could be performed at 120ºC with 70% TFA for 1
352 h to generate 39% RS. To the best of our knowledge, this study is the first approach to
353 mathematically model the thermal and acid hydrolysis of yeast CWs to optimize
354 monosaccharide production experimental conditions. As in the previous study with standards,
355 the time values decreased with an increase in the reaction media acidity. Moreover, the
356 optimal temperature and TFA concentration for obtaining the maximum glucose, mannose
357 and RS concentration from CW was similar: 100ºC/70% TFA, 100ºC/50% TFA and
358 100ºC/70% TFA, respectively. These results confirm the validity of the proposed model and
359 the developed methodology.
360
361 The regression coefficients that relate the temperature to the hydrolysis rates are summarized
362 in Table 6. The correlations between the expected and experimental data were satisfactory (R^2
363 > 0.95) for all cases. The pre-exponential factor for both hydrolysis and decomposition did
364 not show any differences in relation to the increase in the acid percentage used in the reaction.
365 Nevertheless, the increase in acidic conditions generated a small, progressive decrease in the
366 hydrolysis and decomposition activation energies. The Ea_d values for mannose were
367 significantly lower than those obtained in the other cases. This shows that mannose is more
368 sensitive to decomposition due to high temperatures and strong acid conditions.
369
370 *3.4. Modeling the combined effect of temperature and TFA concentration on the hydrolytic*
371 *process*

The joint TFA concentration and temperature effects on the hydrolysis process were also evaluated. As the changes in Ea_h and Ea_d, in relation to the TFA concentrations, were not significant and the k_{h0} and k_{d0} values were quite similar (Tables 3 and 6), we modified the Arrhenius equation to include acid levels in the modeling process [42,43]:

$$k_s = C^{n_s} \exp(a_s) \exp\left(-\frac{Ea_{MS}}{RT}\right) \quad (7)$$

where a_s and n_s are the regression parameters (for $s = h$ or d), C is the TFA concentration (in % v/v), k_s is the kinetic parameter of the combined effect of temperature and acid (for $s = h$ or d), Ea_{MS} is the average of the activation energies (for $s = h$ or d, in kJ/mol), R is the universal gas constant (8.314×10^{-3} kJ mol^{-1} K^{-1}) and T is the absolute temperature (K).

Thus, a global model is defined by inserting equation (7) into equation (2):

$$M = P_0 \frac{C^{n_h} e^{a_h} e^{\left(-\frac{Ea_{Mh}}{RT}\right)}}{C^{n_d} e^{a_d} e^{\left(-\frac{Ea_{Md}}{RT}\right)} - C^{n_h} e^{a_h} e^{\left(-\frac{Ea_{Mh}}{RT}\right)}} \left[\exp\left(-C^{n_h} e^{a_h} \exp\left(-\frac{Ea_{Mh}}{RT}\right)t\right) - \exp\left(-C^{n_d} e^{a_d} \exp\left(-\frac{Ea_{Md}}{RT}\right)t\right)\right] \quad (8)$$

All experimental data from each substrate were fit to this equation (8) to estimate the coefficients a_s and n_s. The activation energies (Ea_{Mh} and Ea_{Md}) were determined as the average of energies showed in Tables 3 and 6 and P_0 was the same previously calculated.

The numerical parameter values obtained from this model are shown in Table 7. Curdlan was the substrate hydrolyzed most easily (lowest Ea_{Mh} value), and its mannose monomers were the most difficult to decompose (highest Ea_{Md} value). The values of coefficients a_s and n_s are in agreement with those reported by other groups that have used a similar mechanistic approach, but worked with different substrate types [39,43-45]. Furthermore, the

397 determination coefficients from the fittings were always higher than 0.93. Finally, hydrolysis
398 kinetics simulations were performed using equation (8) in a range from 50ºC to 130ºC with
399 the TFA concentrations tested in this study (Figure 4). This representation allowed us to
400 predict the kinetic profiles due to the joint effect of temperature and TFA on the hydrolysis of
401 curdlan, mannan and the *E. fibuliger* CW.
402
403 **4. Conclusions**
404 The methods used for CW compositional analysis and the processes developed to produce
405 active oligosaccharides and monosaccharides from complex polysaccharides are based on a
406 chemical reaction in acid media at high temperatures. It is therefore necessary to optimize the
407 effect of these variables (i.e., temperature and acid concentration) on the hydrolysis kinetics.
408 However, the optimal conditions for breaking down curdlan, mannan and yeast CW to obtain
409 the maximum production of glucose and mannose and to avoid the decomposition of these
410 sugars have not yet been determined.
411
412 The experimental results showed that the mannose polymers, both standard and obtained from
413 CWs, were more easily hydrolyzed (i.e., lowest Ea_{Mh} value) than those formed by glucose
414 units. In addition, it was more difficult to destroy mannose than glucose (i.e., highest Ea_{Md}
415 value). The most suitable conditions for maximal sugar release of the three studied substrates
416 are between 50 and 70% TFA at 100ºC, with a processing time interval of between 2.3 and
417 4.58 h. In all of the cases that were assessed, and with both a theoretical and empirical
418 approach, the mathematical modeling of the hydrolysis reactions was statistically significant
419 and consistent, and the equations accurately predicted the experimental profiles.
420
421 **Acknowledgements**
422 Mr. Miguel Angel Prieto Lage was awarded with two grants from the Lucas Labrada and
423 María Barbeito programs financed by the Xunta de Galicia. We wish to thank the CSIC

(Intramural Project: 200930I183) and Xunta de Galicia (Programa de consolidación de unidades de investigación 2008-2010, IN845B-2010/004) for financial support. We are grateful to Dr. Jesús Mirón López for chromatography help. This manuscript has been improved with the comments of five anonymous reviewers. The English usage in the manuscript has been completely revised and edited by AJE language editor.

References

[1] Crognale S, Bruno M, Moresi M, Petruccioli M. Enhanced production of β-glucan from *Botryosphaeria rhodina* using emulsified media or fan impellers. Enzyme Microb Technol, 2007;41:111-20.

[2] Kwiatkowski S, Thielen U, Glenney P, Moran C. A study of *Saccharomyces cerevisiae* cell wall glucans. J Inst Brewing 2009;115:151-8.

[3] Pérez P, Ribas JC. Cell wall analysis. Methods 2004;33:245-51.

[4] Fleet GH, Phaff HJ. Lysis of yeast cell walls: Glucanases from *Bacillus circulans* WL-12. J Bacteriol 1974;119:207-19.

[5] Siwicki AK, Anderson DP, Rumsey GL. Dietary intake of immunostimulants by rainbow trout affects non-specific immunity and protection against furunculosis. Vet Immunol Immunopathol, 1994;41:125-39.

[6] Suphantharika M, Khunrae P, Thanardkit P, Verduyn C. Preparation of spent brewer's yeast β-glucans with a potential application as an immunostimulant for black tiger shrimp, *Penaeus monodon*. Bioresource Technol, 2003;88:55-60.

[7] Figueras A, M. Santarém M, Novoa B. Influence of the sequence of administration of β-glucans and a *Vibrio damsela* vaccine on the immune response of turbot (*Scophthalmus maximus* L.). Vet Immunol Immunopathol 1998;64:59-68.

[8] Volman JJ, Ramakers JD, Plat J. Dietary modulation of immune function by β-glucans. Physiol Behav 2008;94:276-84.

[9] D. Brown G, Siamon G. Fungal β-glucans and mammalian immunity. Cell Press 2003;19:311–5.

[10] El Enshasy H. Immunomodulators. The Mycota (2nd. Edition). Vol X. Springer Verlag; 2010 p. 165-194

[11] Blakeney AB, Harris PJ, Henry RJ, Stone BA. A simple and rapid preparation of alditol acetates for monosaccharide analysis. Carbohydr Res 1983;113:291-9.

[12] Rumpel C, Marie-France Dignac. Gas chromatographic analysis of monosaccharides in a forest soil profile: Analysis by gas cromatography after trifluroacetic acid hydrolysis and reduction-acetylation. Soil Biol Biochem 2006;38:1478-81.

[13] Dallies N, François J, Paquet V. A new method for quantitative determination of polysaccharides in the yeast cell wall. Application to the cell wall defective mutants of *Saccharomyces cerevisiae*. Yeast 1998;14:1297-1306.

[14] Freimund S, Janett S, Arrigoni E, Amadò R. Optimised quantification method for yeast-derived 1,3-β-D-glucan and α-D-mannan. Eur Food Res Technol 2005;220:101-5.

[15] Guilloux-Benatier M, Chassagne D. Comparison of components released by fermented or active dried yeasts after aging on lees in a model wine. J Agric Food Chem 2003;51:746-51.

[16] Solana M, Aznar A. Diseño de un sistema de tratamiento de aguas residuales en una industria de conservas de pescado y marisco. Gestión Ambiental 2002;4:12-21.

[17] Pastrana LM, González MP, Murado MA. Production of gibberellic acid from mussel processing wastes in submerged batch culture. Bioresour Technol 1993;45:213-21.

[18] Murado MA, González MP, Torrado A, Pastrana LM. Amylase production by solid state culture of *Aspergillus oryzae* on polyurethane foams. Some mechanistic approaches from an empirical model. Proc Biochem 1997;32:35-42.

[19] Mirón J, Vázquez JA, González P, Murado MA. Enhancement glucose oxidase production by solid-state fermentation of *Aspergillus niger* on polyurethane foams using mussel processing wastewaters. Enzyme Microb Technol 2010;46:21-7.

[20] Pintado J, Murado MA, González MP, Mirón J, Pastrana L. Joint effect of nitrogen and phosphorus concentrations on citric acid production by different strains of *Aspergillus niger* grown on an effluent. Biotechnol Lett 1993;15:1157-62.

[21] Vázquez Álvarez JA, González MP, Murado MA. Pediocin production by *Pediococcus acidilactici* in solid state culture on a waste medium: Process simulation and experimental results. Biotechnol Bioeng 2004;85:676-82.

[22] Vázquez JA, Montemayor MI, Fraguas J, Murado MA. Hyaluronic acid production by *Streptococcus zooepidemicus* in marine by-products media from mussel processing wastewaters and tuna peptone viscera. Microb Cell Fact 2010;9:46.

[23] González MP, Mirón J, Murado MA. Culture of *Endomyces fibuliger* in mussel processing wastes and precipitation with PEGs of its extracellular amylolytic system. Biotechnol Lett 1987;9:281-6.

[24] Nguyen TH, Fleet GH, Rogers PL. Composition of cell walls of several yeast species. Appl Microbiol Biotechnol 1998;50:206-12.

[25] Murado MA, González MP, Pastrana L, Siso MIG, Mirón J, Montemayor MI. Enhancement of the bioproduction potential of an amylaceous effluent. Bioresour Technol 1993;44:155-63.

[26] González MªP, Siso MªIG, Murado MA, Pastrana L, Montemayor MªI, Mirón J. Depuration and valuation of mussel-processing wastes. Characterization of amylolytic postincubates from different species grown on an effluent. Bioresour Technol 1992;42:133-40.

[27] Pintado J, González MP and Murado MA. Interactions between pretreatment and nutrient concentrations of mussel processing effluents for citric acid production. Enzyme Microb Tech 1997;20:544-9

[28] Dubois M, Gilles KA, Hamilton JK, Rebers PA, Smith F. Colorimetric method for determination of sugars and related substances. Anal Chem 1956;28:350-6.

[29] Strickland JDH, Parsons TR. A practical handbook of sea water analysis. Bull Fish Res Board Can 1968;167:57-62.

[30] Lowry OH, Rosebrough NJ, Farr AL, Randall RJ. Protein measurement with the Folin phenol reagent. J Biol Chem 1951;193:265-75.

[31] Havilah EJ, Wallis DM, Morris R, Woolnough JA. A microcolorimetric method for determination of ammonia in Kjeldahl digests with a manual spectrophotometer. Lab Pract 1977;545-7.

[32] Bernfeld P. Enzymes of starch degradation and synthesis. Adv Enzymol 1951;12:379-427.

[33] Manirakiza P, Covaci A, Schepens P. Comparative study on total lipid determination using soxhlet, roese-gottlieb, bligh & dyer, and modified bligh & dyer extraction methods. J. Food Comp Anal 2000;14:93-100.

[34] Kasahara S. Involvement of cell wall β-glucan in the action of HM-1 killer toxin. FEBS Lett 1994;348:27-32.

[35] Whiton RS, Lau P, Morgan SL. Modification in the alditol acetate method for analysis of muramic acid and other neutral and amino sugars by capillary gas chromatography-mass spectrometry with selected ion monitoring. J Chromatogr 1985;347:109-20.

[36] Osborn HMI, Lochey F, Mosley L, Read D. Analysis of polysaccharides and monosaccharides in the root mucilege of maize (*Zea mays* L.) by gas cromatography. J Chromatogr 1999;831:267-76.

[37] Saeman JF. Kinetics of wood saccharification. Hydrolysis of cellulose and decomposition of sugars in dilute acid at high temperature. Industr Eng Chem 1945;37:43-52.

[38] Maloney MT, Chapman TW, Baker AJ. Dilute acid hydrolysis of paper birch: Kinetics studies of xylan and acetyl-group hydrolysis. Biotechnol Bioeng 1985;27:355-61.

[39] Rodríguez-Chong A, Ramírez JA, Garrote G, Vázquez M. Hydrolysis of sugar cane bagasse using nitric acid: A kinetic assessment. J Food Eng 2004;61:143-52.

[40] Choi CH, Mathews AP. Two-step acid hydrolysis process kinetics in the saccharification of low-grade biomass: 1. Experimental studies on the formation and degradation of sugars. Bioresour Technol 1996;58:101-6.

[41] Dallies N, Francois J, Paquet V. A new method for quantitative determination of polysaccharides in the yeast cell wall. Application to the cell wall defective mutants of *Saccharomyces cerevisae*. Yeast 1998;14:1297-306.

[42] Srinivasan R, MacDonald DG, Bakhshi NN. Kinetic studies of wheat straw hydrolysis using sulphuric acid. Can J Chem Eng 1983;63:840-4.

[43] Aguilar R, Ramírez JA, Garrote G, Vázquez M. Kinetic study of the acid hydrolysis of sugar cane bagasse. J Food Eng 2002;55:309-18.

[44] He P-, Lü F, Shao L-, Pan X-, Lee D-. Kinetics of enzymatic hydrolysis of polysaccharide-rich particulates. J Chin Inst Chem Eng 2007;38:21-7.

[45] Arnous A, Meyer AS. Quantitative prediction of cell wall polysaccharide composition in grape (*Vitis vinifera* L.) and apple (*Malus domestica*) skins from acid hydrolysis monosaccharide profiles. J Agric Food Chem 2009;57:3611-3619.

Figure Captions

Figure 1: Time course of *E. fibuliger* culture on MPW-based medium. X: biomass (▲); Pr: proteins (○); Gl: glycogen (●); RS: reducing sugars (△); TAA: total amylolytic activity (◆) and pH (■). Error bars are the confidence intervals (α=0.05, n=2).

Figure 2: The kinetics of glucose and mannose released (%) from the hydrolysis of polysaccharides mannan and curdlan at different temperatures (▲: 35ºC; ●: 80ºC; △: 100ºC; ○: 120ºC) and concentrations of TFA (%). The experimental data (points) were fit to equation (2) (solid lines). For clarity, confidence intervals (in all cases less than 5% of the experimental mean value; α=0.05; n=2) were omitted.

Figure 3: The kinetics of glucose, mannose and reducing sugars released (%) from *E. fibuliger* CW hydrolysis at different temperatures (▲: 35ºC; ●: 80ºC; △: 100ºC; ○: 120ºC) and concentrations of TFA (%). The experimental data (points) were fit to equation (2) (solid lines). For clarity, confidence intervals (in all cases less than 5% of the experimental mean value; α=0.05; n=2) were omitted.

Figure 4: Simulations of monosaccharide hydrolysis kinetics by equation (8) at different temperatures and TFA concentrations in the curdlan, mannan and CW substrates. 1: 130ºC; 2: 120ºC; 3: 110ºC; 4: 100ºC; 5: 90ºC; 6: 80ºC; 7: 70ºC; 8: 60ºC; 9: 50ºC. For clarity, confidence intervals (in all cases less than 5% of the experimental mean value; α=0.05; n=2) were omitted.

Table Captions

Table 1: Kinetic parameter values for equation (2) that describing the hydrolysis process of curdlan and mannan at different temperatures and TFA concentrations. Values ± Confidence Intervals for α=0.05; *p*-value from Fisher´s *F*-test (α=0.05); R^2: determination coefficients between experimental and predicted data; (-): zero value was obtained. NS: not significant.

Table 2: Numerical values of time for achieving the maximum monosaccharides concentration (t_m) and maximum monosaccharides concentration (M_m) at the different temperatures and TFA concentrations tested. These values were calculated using equations (3) and (4) with the parameters summarized in Table 1. (-): no value was obtained.

Table 3: Effect of temperature on the kinetic parameters (k_h and k_d) shown in Table 1 for curdlan and mannan hydrolysis. The bivariate equation (6) was used to fit these parameters. Values ± Confidence Intervals for α=0.05; *p*-value from Fisher´s *F*-test (α=0.05); R^2: determination coefficients between experimental and predicted data. NS: not significant.

Table 4: Kinetic parameters values for equation (2), which describes the hydrolysis process of *E. fibuliger* CW at different temperatures and TFA concentrations. The dependent variables were glucose, mannose and reducing sugars as measured by GC-MS and spectrophotometry, respectively. Values ± Confidence Intervals for α=0.05; *p*-value from Fisher´s *F*-test (α=0.05); R^2: determination coefficients between experimental and predicted data; (-): zero value was obtained. NS: not significant.

Table 5: Numerical values of the time for achieving the maximum monosaccharides concentration (t_m) and maximum monosaccharides concentration (M_m) at the different temperatures and TFA concentrations tested. These values were calculated using equations (3) and (4) with the parameters summarized in Table 4. (-): no value was obtained.

Table 6: Effect of temperature on the kinetic parameters (k_h and k_d) shown in Table 4 for the hydrolysis of *E. fibuliger* CW. The bivariate equation (6) has been employed to fit these parameters. Values ± Confidence Intervals for α=0.05; *p*-value from Fisher´s *F*-test (α=0.05); R^2: determination coefficients between experimental and predicted data. NS: not significant.

Table 7: Numerical estimates obtained using equation (8). Values ± Confidence Intervals for α=0.05; *p*-value from Fisher´s *F*-test (α=0.05); R^2: determination coefficients between experimental and predicted data.

TABLES

Table 1

	TFA (%)				
PARAMETERS	**10**	**20**	**35**	**50**	**70**
CURDLAN					
P_0 (%)	100 ± 2.79	100 ± 2.79	100 ± 2.79	100 ± 2.79	100 ± 2.79
k_h (h^{-1})–T=35ºC	1×10^{-20} (NS)	1×10^{-20} (NS)	6×10^{-5} (NS)	7×10^{-6} (NS)	7×10^{-5} (NS)
k_h (h^{-1})–T=80ºC	0.010 ± 0.005	0.058 ± 0.008	0.093 ± 0.012	0.320 ± 0.043	0.550 ± 0.095
k_h (h^{-1})–T=100ºC	0.060 ± 0.009	0.330 ± 0.047	0.500 ± 0.083	1.291 ± 0.540	1.897 ± 0.196
k_h (h^{-1})–T=120ºC	0.244 ± 0.036	0.671 ± 0.148	1.298 ± 0.660	2.879 ± 0.513	5.200 ± 1.916
k_d (h^{-1})–T=35ºC	5.8×10^{-4} (NS)	5.8×10^{-4} (NS)	5.8×10^{-4} (NS)	5.8×10^{-4} (NS)	5.8×10^{-4} (NS)
k_d (h^{-1})–T=80ºC	0.003 ± 0.002	0.004 ± 0.003	0.005 ± 0.003	0.004 ± 0.002	0.002 ± 0.000
k_d (h^{-1})–T=100ºC	0.014 ± 0.005	0.005 ± 0.002	0.013 ± 0.002	0.018 ± 0.003	0.027 ± 0.003
k_d (h^{-1})–T=120ºC	0.046 ± 0.006	0.053 ± 0.006	0.103 ± 0.012	0.133 ± 0.012	0.240 ± 0.070
R^2	0.967	0.993	0.995	0.986	0.992
p-values	<0.001	<0.001	<0.001	<0.001	<0.001
MANNAN					
P_0 (%)	100 ± 3.68	100 ± 3.68	100 ± 3.68	100 ± 3.68	100 ± 3.68
k_h (h^{-1})–T=35ºC	2.6×10^{-5} (NS)	4.8×10^{-6} (NS)	4.8×10^{-6} (NS)	2.8×10^{-6} (NS)	4.8×10^{-6} (NS)
k_h (h^{-1})–T=80ºC	0.025 ± 0.006	0.045 ± 0.008	0.172 ± 0.022	0.321 ± 0.047	0.197 ± 0.026
k_h (h^{-1})–T=100ºC	0.129 ± 0.017	0.161 ± 0.022	0.689 ± 0.147	1.402 ± 0.692	2.282 ± 1.293
k_h (h^{-1})–T=120ºC	0.580 ± 0.132	0.573 ± 0.130	1.819 ± 0.380	2.996 ± 2.160	5.438 ± 0.434
k_d (h^{-1})–T=35ºC	6.8×10^{-6} (NS)	6.8×10^{-6} (NS)	6.8×10^{-6} (NS)	6.8×10^{-6} (NS)	6.8×10^{-6} (NS)
k_d (h^{-1})–T=80ºC	0.001 ± 0.000	0.005 ± 0.001	0.006 ± 0.003	0.005 ± 0.003	0.017 ± 0.004
k_d (h^{-1})–T=100ºC	0.026 ± 0.005	0.029 ± 0.005	0.031 ± 0.005	0.040 ± 0.006	0.087 ± 0.015
k_d (h^{-1})–T=120ºC	0.160 ± 0.022	0.164 ± 0.022	0.162 ± 0.026	0.192 ± 0.052	0.500 ± 0.210
R^2	0.984	0.990	0.994	0.993	0.990
p-values	<0.001	<0.001	<0.001	<0.001	<0.001

Table 2

	TFA (%)				
PARAMETERS	**10**	**20**	**35**	**50**	**70**
CURDLAN					
t_m **(h)–T=35ºC**	-	-	-	-	-
M_m **(%)–T=35ºC**	-	-	-	-	-
t_m **(h)–T=80ºC**	173.88	48.84	33.47	14.20	10.74
M_m **(%)–T=80ºC**	59.67	81.19	85.02	94.76	98.42
t_m **(h)–T=100ºC**	31.74	12.59	7.56	3.37	2.28
M_m **(%)–T=100ºC**	64.06	93.57	90.72	94.23	94.10
t_m **(h)–T=120ºC**	8.45	4.10	2.12	1.12	0.62
M_m **(%)–T=120ºC**	67.88	80.36	80.39	86.17	86.17
MANNAN					
t_m **(h)–T=35ºC**	-	-	-	-	-
M_m **(%)–T=35ºC**	-	-	-	-	-
t_m **(h)–T=80ºC**	144.03	54.92	20.09	13.10	13.69
M_m **(%)–T=80ºC**	89.07	76.25	88.35	93.78	79.47
t_m **(h)–T=100ºC**	15.54	12.83	4.70	2.60	1.49
M_m **(%)–T=100ºC**	66.40	69.05	86.34	90.00	87.83
t_m **(h)–T=120ºC**	3.05	3.07	1.48	0.98	0.48
M_m **(%)–T=120ºC**	61.08	60.45	79.41	82.87	78.53

Table 3

PARAMETERS	TFA (%) 10	20	35	50	70
CURDLAN					
Ea_h (kJ/mol)	74.49 ± 13.79	71.25 ± 12.74	69.2 ± 13.13	66.55 ± 9.74	64.71 ± 8.85
k_{h0} (h^{-1})	2×10^9 (NS)	2×10^9 (NS)	2×10^9 (NS)	2×10^9 (NS)	2×10^9 (NS)
Ea_d (kJ/mol)	119.3 ± 72.7	118.0 ± 40.9	117.0 ± 26.5	115.9 ± 24.1	114.0 ± 19.7
k_{d0} (h^{-1})	3×10^{14} (NS)	3×10^{14} (NS)	3×10^{14} (NS)	3×10^{14} (NS)	3×10^{14} (NS)
R^2	0.941	0.979	0.977	0.954	0.962
p-values	<0.001	<0.001	<0.001	<0.001	<0.001
MANNAN					
Ea_h (kJ/mol)	71.99 ± 19.55	71.98 ± 19.60	68.11 ± 17.04	66.40 ± 13.19	64.53 ± 13.11
k_{h0} (h^{-1})	2×10^9 (NS)	2×10^9 (NS)	2×10^9 (NS)	2×10^9 (NS)	2×10^9 (NS)
Ea_d (kJ/mol)	115.3 ± 38.5	115.2 ± 38.3	115.3 ± 32.3	114.7 ± 29.2	111.6 ± 23.4
k_{d0} (h^{-1})	3×10^{14} (NS)	3×10^{14} (NS)	3×10^{14} (NS)	3×10^{14} (NS)	3×10^{14} (NS)
R^2	0.970	0.987	0.974	0.953	0.983
p-values	<0.001	<0.001	<0.001	<0.001	<0.001

Table 4

	TFA (%)				
PARAMETERS	**10**	**20**	**35**	**50**	**70**
GLUCOSE as dependent variable					
P_0 (%)	41.0 ± 5.0	41.0 ± 5.0	41.0 ± 5.0	41.0 ± 5.0	41.0 ± 5.0
k_h (h^{-1})–T=35ºC	1.3×10^{-3} (NS)	8×10^{-4} (NS)	1×10^{-3} (NS)	8.6×10^{-4} (NS)	2.5×10^{-3} (NS)
k_h (h^{-1})–T=80ºC	0.016 ± 0.010	0.020 ± 0.011	0.028 ± 0.012	0.049 ± 0.015	0.093 ± 0.022
k_h (h^{-1})–T=100ºC	0.062 ± 0.018	0.151 ± 0.037	0.188 ± 0.047	0.204 ± 0.052	0.589 ± 0.219
k_h (h^{-1})–T=120ºC	0.236 ± 0.068	0.429 ± 0.140	0.543 ± 0.219	0.612 ± 0.290	2.258 ± 0.139
k_d (h^{-1})–T=35ºC	1.5×10^{-5} (NS)	1.4×10^{-6} (NS)	1.4×10^{-6} (NS)	7.5×10^{-6} (NS)	7.5×10^{-6} (NS)
k_d (h^{-1})–T=80ºC	0.015 ± 0.000	0.025 ± 0.003	0.035 ± 0.024	0.043 ± 0.016	0.039 ± 0.011
k_d (h^{-1})–T=100ºC	0.026 ± 0.007	0.078 ± 0.012	0.053 ± 0.013	0.053 ± 0.013	0.049 ± 0.013
k_d (h^{-1})–T=120ºC	0.152 ± 0.029	0.204 ± 0.048	0.321 ± 0.075	0.437 ± 0.110	0.460 ± 0.448
R^2	0.963	0.961	0.978	0.991	0.990
p-values	<0.001	<0.001	<0.001	<0.001	<0.001
MANNOSE as dependent variable					
P_0 (%)	24.5 ± 1.5	24.5 ± 1.5	24.5 ± 1.5	24.5 ± 1.5	24.5 ± 1.5
k_h (h^{-1})–T=35ºC	1.7×10^{-3} (NS)	4.3×10^{-3} (NS)	4.1×10^{-3} (NS)	3.4×10^{-3} (NS)	4.1×10^{-3} (NS)
k_h (h^{-1})–T=80ºC	0.022 ± 0.010	0.030 ± 0.011	0.036 ± 0.011	0.084 ± 0.017	0.150 ± 0.029
k_h (h^{-1})–T=100ºC	0.124 ± 0.024	0.335 ± 0.072	0.629 ± 0.180	0.790 ± 0.260	0.852 ± 0.310
k_h (h^{-1})–T=120ºC	0.579 ± 0.179	0.981 ± 0.492	2.384 ± 1.300	2.835 ± 0.011	3.145 ± 0.027
k_d (h^{-1})–T=35ºC	1.5×10^{-5} (NS)	3.2×10^{-3} (NS)	3.4×10^{-3} (NS)	1×10^{-11} (NS)	3.9×10^{-7} (NS)
k_d (h^{-1})–T=80ºC	0.015 ± 0.000	0.013 ± 0.002	0.016 ± 0.013	0.021 ± 0.007	0.040 ± 0.009
k_d (h^{-1})–T=100ºC	0.026 ± 0.007	0.025 ± 0.006	0.032 ± 0.007	0.037 ± 0.008	0.055 ± 0.011
k_d (h^{-1})–T=120ºC	0.152 ± 0.029	0.205 ± 0.038	0.298 ± 0.189	0.371 ± 0.192	0.461 ± 0.248
R^2	0.953	0.954	0.978	0.989	0.989
p-values	<0.001	<0.001	<0.001	<0.001	<0.001
REDUCING SUGARS as dependent variable					
P_0 (%)	56.6 ± 3.7	56.6 ± 3.7	56.6 ± 3.7	56.6 ± 3.7	56.6 ± 3.7
k_h (h^{-1})–T=35ºC	4.3×10^{-4} (NS)	2.2×10^{-4} (NS)	7×10^{-4} (NS)	1.5×10^{-4} (NS)	3.6×10^{-3} (NS)
k_h (h^{-1})–T=80ºC	0.030 ± 0.009	0.053 ± 0.012	0.072 ± 0.014	0.102 ± 0.016	0.173 ± 0.026
k_h (h^{-1})–T=100ºC	0.154 ± 0.023	0.328 ± 0.053	0.477 ± 0.090	0.602 ± 0.130	1.150 ± 0.460
k_h (h^{-1})–T=120ºC	0.411 ± 0.086	0.834 ± 0.279	1.126 ± 0.621	1.064 ± 0.590	2.054 ± 0.580
k_d (h^{-1})–T=35ºC	3.2×10^{-3} (NS)	3.2×10^{-3} (NS)	3.2×10^{-3} (NS)	3.2×10^{-3} (NS)	3.2×10^{-3} (NS)
k_d (h^{-1})–T=80ºC	0.013 ± 0.001	0.023 ± 0.009	0.029 ± 0.008	0.018 ± 0.005	0.021 ± 0.005
k_d (h^{-1})–T=100ºC	0.021 ± 0.005	0.019 ± 0.004	0.022 ± 0.004	0.028 ± 0.005	0.029 ± 0.005
k_d (h^{-1})–T=120ºC	0.081 ± 0.013	0.135 ± 0.020	0.214 ± 0.033	0.276 ± 0.044	0.380 ± 0.330
R^2	0.980	0.991	0.988	0.989	0.985
p-values	<0.001	<0.001	<0.001	<0.001	<0.001

Table 5

	TFA (%)				
PARAMETERS	**10**	**20**	**35**	**50**	**70**
GLUCOSE as variable dependent					
t_m **(h)–T=35ºC**	-	-	-	-	-
M_m **(%)–T=35ºC**	-	-	-	-	-
t_m **(h)–T=80ºC**	56.83	44.17	31.94	21.84	16.14
M_m **(%)–T=80ºC**	13.55	13.55	13.30	16.09	22.00
t_m **(h)–T=100ºC**	17.15	11.13	9.38	8.95	4.58
M_m **(%)–T=100ºC**	17.07	24.06	24.91	25.58	32.74
t_m **(h)–T=120ºC**	5.45	3.30	2.37	1.93	0.88
M_m **(%)–T=120ºC**	19.21	20.91	19.16	17.69	27.30
MANNOSE as variable dependent					
t_m **(h)–T=35ºC**	-	-	-	-	-
M_m **(%)–T=35ºC**	-	-	-	-	-
t_m **(h)–T=80ºC**	54.74	48.98	40.13	21.88	12.04
M_m **(%)–T=80ºC**	10.79	12.80	12.77	15.35	15.15
t_m **(h)–T=100ºC**	15.94	8.41	5.00	4.08	3.44
M_m **(%)–T=100ºC**	16.22	19.89	20.88	21.06	20.27
t_m **(h)–T=120ºC**	3.13	2.02	1.00	0.83	0.72
M_m **(%)–T=120ºC**	15.21	16.19	18.20	18.03	17.61
REDUCING SUGARS as variable dependent					
t_m **(h)–T=35ºC**	-	-	-	-	-
M_m **(%)–T=35ºC**	-	-	-	-	-
t_m **(h)–T=80ºC**	49.74	27.74	21.07	20.80	13.85
M_m **(%)–T=80ºC**	30.25	29.81	30.71	39.11	42.24
t_m **(h)–T=100ºC**	15.02	9.23	6.78	5.36	3.27
M_m **(%)–T=100ºC**	41.31	47.57	48.84	48.81	51.42
t_m **(h)–T=120ºC**	4.93	2.61	1.82	1.71	1.01
M_m **(%)–T=120ºC**	38.05	39.84	38.34	35.27	38.60

Table 6

PARAMETERS	TFA (%) 10	20	35	50	70
GLUCOSE as variable dependent					
Ea_h (kJ/mol)	84.93 ± 21.73	83.10 ± 19.64	81.84 ± 21.27	81.46 ± 23.06	77.27 ± 21.83
k_{h0} (h^{-1})	4×10^{10} (NS)	4×10^{10} (NS)	4×10^{10} (NS)	4×10^{10} (NS)	4×10^{10} (NS)
Ea_d (kJ/mol)	115.6 ± 50.9	114.5 ± 35.6	113.0 ± 33.0	112.0 ± 33.2	111.9 ± 23.3
k_{d0} (h^{-1})	3×10^{14} (NS)	3×10^{14} (NS)	3×10^{14} (NS)	3×10^{14} (NS)	3×10^{14} (NS)
R^2	0.954	0.989	0.993	0.990	0.990
p-values	<0.001	<0.001	<0.001	<0.001	<0.001
MANNOSE as variable dependent					
Ea_h (kJ/mol)	81.74 ± 27.11	79.92 ± 30.55	77.10 ± 30.58	76.52 ± 28.30	76.19 ± 26.97
k_{h0} (h^{-1})	4×10^{10} (NS)	4×10^{10} (NS)	4×10^{10} (NS)	4×10^{10} (NS)	4×10^{10} (NS)
Ea_d (kJ/mol)	94.03 ± 45.87	93.10 ± 37.51	91.89 ± 28.31	91.18 ± 26.28	90.46 ± 25.12
k_{d0} (h^{-1})	5×10^{11} (NS)	5×10^{11} (NS)	5×10^{11} (NS)	5×10^{11} (NS)	5×10^{11} (NS)
R^2	0.992	0.986	0.984	0.982	0.981
p-values	<0.001	<0.001	<0.001	<0.001	<0.001
REDUCING SUGARS as variable dependent					
Ea_h (kJ/mol)	80.48 ± 17.00	78.15 ± 19.01	77.15 ± 21.31	77.21 ± 21.91	75.07 ± 20.24
k_{h0} (h^{-1})	2×10^{10} (NS)	2×10^{10} (NS)	2×10^{10} (NS)	2×10^{10} (NS)	2×10^{10} (NS)
Ea_d (kJ/mol)	119.9 ± 53.1	118.2 ± 34.8	116.8 ± 29.2	115.9 ± 28.3	114.9 ± 24.8
k_{d0} (h^{-1})	7×10^{14} (NS)	7×10^{14} (NS)	7×10^{14} (NS)	7×10^{14} (NS)	7×10^{14} (NS)
R^2	0.989	0.977	0.979	0.993	0.989
p-values	<0.001	<0.001	<0.001	<0.001	<0.001

Table 7

	CURDLAN	MANNAN	CW (Glucose)	CW (Mannose)	CW (RS)
Ea_{Mh} (kJ/mol)	69.78 ± 0.05	70.03 ± 0.02	82.32 ± 0.16	79.92 ± 0.23	70.68 ± 0.11
a_h	16.14 ± 0.01	15.48 ± 0.01	15.10 ± 0.05	22.38 ± 0.07	18.74 ± 0.03
n_h	1.63 ± 0.00	1.79 ± 0.00	2.56 ± 0.00	0.77 ± 0.00	0.84 ± 0.00
Ea_{Md} (kJ/mol)	114.07 ± 0.08	117.27 ± 0.06	113.25 ± 0.20	92.63 ± 0.23	115.03 ± 0.23
a_d	29.69 ± 0.02	29.48 ± 0.02	31.33 ± 0.06	24.97 ± 0.07	30.77 ± 0.07
n_d	1.03 ± 0.00	1.16 ± 0.00	0.61 ± 0.01	0.60 ± 0.00	0.81 ± 0.01
R^2	0.983	0.992	0.946	0.980	0.931
p-values	<0.001	<0.001	<0.001	<0.001	<0.001

FIGURES

Figure 1

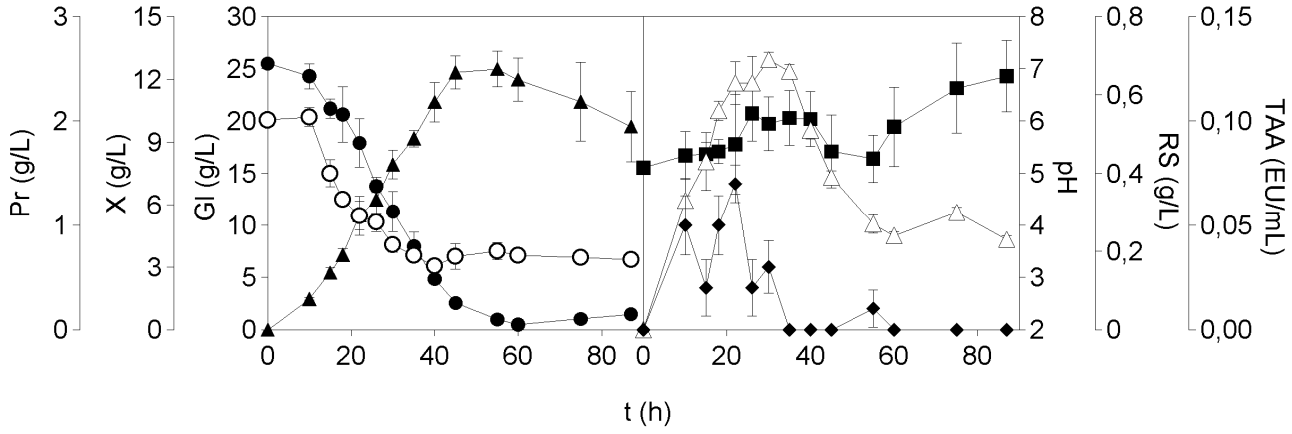

Figure 2

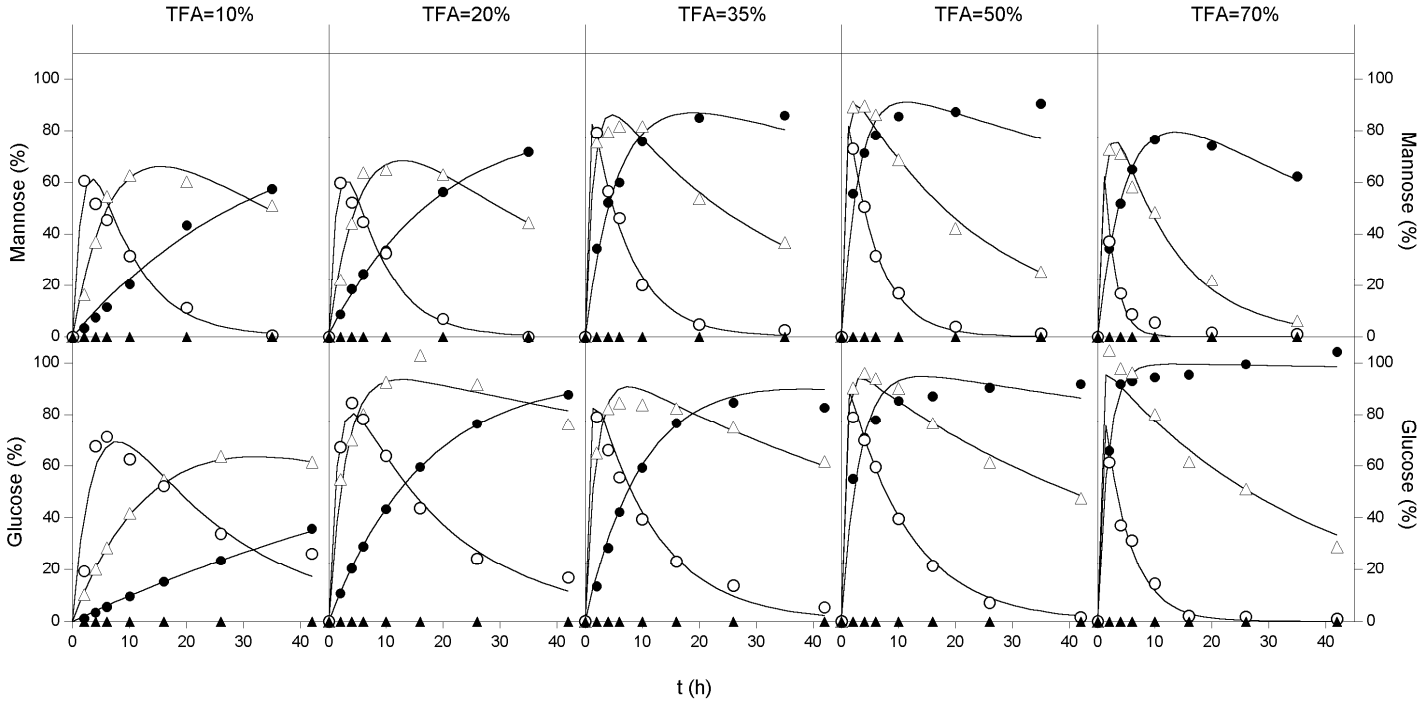

Figure 3

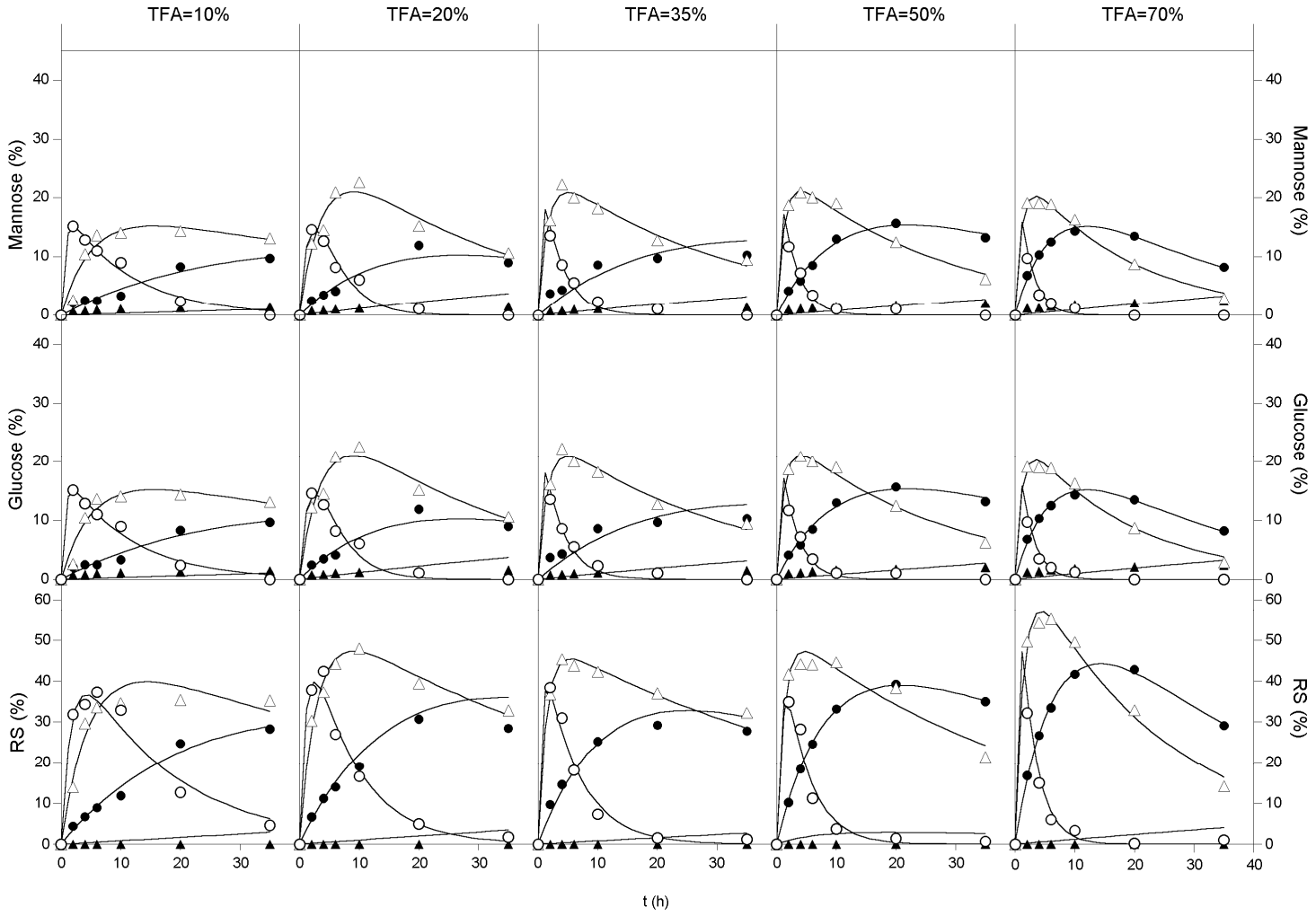

Figure 4

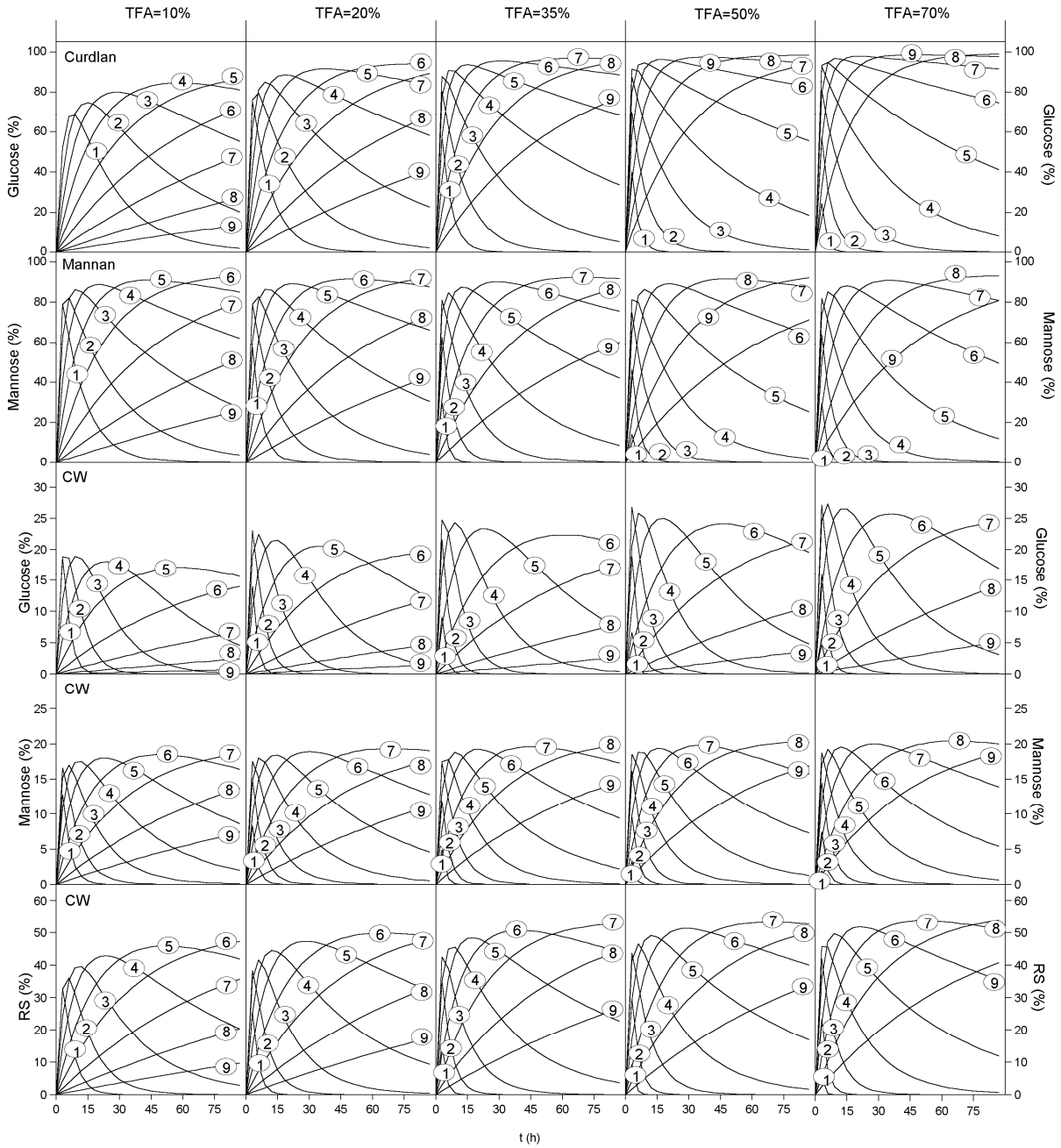
TFA=10%
TFA=20%
TFA=35%
TFA=50%
TFA=70%
Curdlan
Mannan
CW
CW
CW
Glucose (%)
Mannose (%)
RS (%)
t (h)